ARTICLE

Analytical Solution for the Convectively-Mixed Atmospheric Boundary Layer

H. G. Ouwersloot · J. Vilà-Guerau de Arellano

Abstract Based on the prognostic equations of mixed-layer theory assuming a zeroth order jump at the entrainment zone, analytical solutions for the boundary-layer height evolution are derived with different degrees of accuracy. First, an exact implicit expression for the boundary-layer height for a situation without moisture is analytically derived without assuming any additional relationships or specific initial conditions. It is shown that to expand the solution to include moisture, only minor approximations have to be made. Second, for relatively large boundary-layer heights, the implicit representation is simplified to an explicit function. Third, a hybrid expression is proposed as a reasonable representation for the boundary-layer height evolution during the entire day. Subsequently, the analysis is extended to present the evolution of any boundary-layer averaged scalar, either inert or under idealized chemistry, as an analytical function of time and boundary-layer height. Finally, the analytical solutions are evaluated. This evaluation includes a sensitivity analysis of the boundary-layer height for the entrainment ratio, the free tropospheric lapse rate of the potential temperature, the time-integrated surface flux and the initial boundary-layer height and potential temperature jump.

Keywords Analytical solution · Boundary-layer height evolution · Mixed-layer theory · Prognostic equations

H. G. Ouwersloot (✉) · J. Vilà-Guerau de Arellano
Meteorology and Air Quality Section, Wageningen University, Wageningen, The Netherlands
e-mail: huug.ouwersloot@wur.nl

J. Vilà-Guerau de Arellano
e-mail: jordi.vila@wur.nl

H. G. Ouwersloot
Max Planck Institute for Chemistry, Mainz, Germany

List of Symbols

h	Boundary-layer height
q	Specific humidity
θ	Potential temperature
θ_v	Virtual potential temperature
$\overline{w'q'}$	Vertical kinematic moisture flux
$\overline{w'\theta'}$	Vertical kinematic heat flux
$\overline{w'\theta'_v}$	Buoyancy flux
c_p	Specific heat capacity of air
D_0	Initial temperature deficit
$D_{v,0}$	Initial virtual temperature deficit
I	Time-integrated surface buoyancy flux
Q	Heat
t	Time
z_0	Roughness length
α	Accuracy
β	Entrainment constant
ρ	Density of dry air
ϕ	Conserved scalar
$\langle\psi\rangle$	Mixed-layer average of arbitrary variable ψ
ψ_{FT}	Value of ψ in the free troposphere
$\Delta\psi$	Jump of ψ at the inversion, $\psi_{FT} - \langle\psi\rangle$
γ_ψ	Free tropospheric gradient of ψ
$\overline{w'\psi'}_0$	Vertical kinematic surface flux of ψ
$\overline{w'\psi'}_h$	Vertical kinematic entrainment flux of ψ
$\hat{H}$	Dimensionless boundary-layer height
$\hat{J}$	Dimensionless virtual potential temperature jump at the inversion
$\hat{F}$	Dimensionless surface buoyancy flux

1 Introduction

The evolution of the atmospheric boundary layer (ABL) has been the subject of study for decades, since this region is the part of the atmosphere that is directly influenced by the presence of the earth's surface (Stull 1988; Garratt 1992). For the convective boundary layer (CBL), which is common during daytime conditions over land, prognostic equations have been derived by Lilly (1968) to calculate the CBL height, the potential temperature and the inversion between the ABL and the free troposphere for maritime conditions. These equations, based on mixed-layer theory, have been further expanded since (Betts 1973; Carson 1973; Tennekes 1973). The prognostic equations enable a conceptual view of the CBL to identify acting processes and study their interactions.

The system of equations resulted in the development of mixed-layer models, which are numerical models that, based on the available boundary and initial conditions, predict the evolution of the boundary-layer dynamics. The mixed-layer models have been applied to study multiple individual processes such as interactions between land and the atmosphere (e.g., de Bruin 1983; van Heerwaarden et al. 2010), the onset of clouds (Ek and Holtslag 2004), the impact of entrainment on carbon dioxide concentrations (Culf et al. 1997) and

the influence of both non-stationary surface fluxes (van Driel and Jonker 2011) and elevated residual layers (Stensrud 1993) on the boundary-layer evolution. Furthermore, mixed-layer theory has been employed to interpret observational data, e.g. for the DOMINO, Diel Oxidant Mechanisms in relation to Nitrogen Oxides (van Stratum et al. 2012) and HUMPPA-COPEC-2010, Hyytiälä United Measurement of Photochemistry and Particles Comprehensive Organic Particle and Environmental Chemistry—2010 (Ouwersloot et al. 2012) campaigns.

Using the mixed-layer model, it has been demonstrated that boundary-layer dynamics and, in particular, the evolution of the boundary-layer height can significantly affect atmospheric chemistry (e.g., Vilà-Guerau de Arellano et al. 2009). This shows that an accurate knowledge of the evolution of boundary-layer dynamics is valuable and that an analytical expression for this evolution is relevant and useful to determine how these dynamics govern the diurnal variability of the thermodynamic variables and the atmospheric constituents such as carbon dioxide (e.g., Pino et al. 2012). Analytical expressions allow for extra insight into the driving processes by identifying dimensionless variables and expressing the boundary-layer height evolution as a function of these variables. Additionally, the analytical expressions provide continuous functions for the sensitivities of the boundary-layer properties to the different initial and boundary conditions. As a consequence, the expressions enable us to identify the distinct phases in the boundary-layer height evolution and quantify when those phases occur.

To the authors' knowledge, no complete analytical solutions including the effect of humidity have been published yet without assuming specific initial conditions. Most presented solutions (e.g., Carson 1973; Garratt 1992) neglect the non-linear dependence of the potential temperature jump at the inversion on the boundary-layer height. A complete analytical expression for a situation without moisture is presented by Driedonks (1982). In his manuscript its derivation is not shown, but it is important to note that his expression can only be obtained when this non-linear dependence is included. Here we independently obtain the same analytical solution and in addition include the effects of specific humidity. We further complete the study by presenting the evolutions of inert species concentrations and the accuracy of the explicit simplification for the boundary-layer height. Additionally, we performed a sensitivity analysis for the final boundary-layer height as a function of the driving initial and boundary conditions. The influence of subsidence is not taken into account, as is common for the published analytical solutions, with the exception of Carson (1973). It will be shown that, by adding subsidence, no solution for the equations can be derived with the applied mathematical techniques.

For the sake of clarity, the solutions and their implications are discussed in the main text, while the full derivations are given in the Appendix. First, we introduce the prognostic equations for the convectively mixed boundary layer without including the moisture effects. Special emphasis is put on the role of the initial conditions and the non-linear dependence of the potential temperature on the boundary-layer height. Subsequently, we discuss the derivation of the analytical solutions for a convective boundary layer without specific humidity. After that, we show the modification of the solutions due to the specific humidity. We then extend the analysis to express how the evolution of the scalars in the CBL responds to the evolution of the boundary-layer dynamics. These scalars include chemical species for idealized chemistry. Finally, the derived relationships are evaluated and an improved explicit approximation of the boundary-layer height evolution is presented. The evaluation includes an analysis of the sensitivity of the final boundary-layer height to the variables that govern its evolution.

2 Results

2.1 Governing Equations

The governing equations for boundary-layer dynamics without including moisture can be derived from the conservation of heat. In this derivation it is assumed that the vertical profiles of conservative scalars (e.g., potential temperature and specific humidity) are characterized by a uniform value with height, $\langle\theta\rangle$, in the boundary layer, a discontinuity, $\Delta\theta$, in an infinitesimally thin inversion layer at the top of the boundary layer and a constant vertical gradient with height and in time, γ_θ, in the free tropospheric layer aloft. This assumption, as well as the resulting governing equations for a case without moisture, were previously presented by Tennekes (1973). The governing equations for a situation without the influence of subsidence, cloud processes (e.g. radiation and phase changes) or advection read

$$\frac{dh}{dt} = -\frac{\overline{w'\theta'}_h}{\Delta\theta}, \tag{1}$$

$$\frac{d\langle\theta\rangle}{dt} = \frac{\overline{w'\theta'}_0 - \overline{w'\theta'}_h}{h}, \tag{2}$$

$$\frac{d\Delta\theta}{dt} = \gamma_\theta \frac{dh}{dt} - \frac{d\langle\theta\rangle}{dt}, \tag{3}$$

where h is the boundary-layer height, characterized by extremes in the vertical fluxes and discontinuities in the vertical profiles, $\overline{w'\theta'}_0$ is the Reynolds-averaged surface heat flux, which here is considered to be prescribed, and $\overline{w'\theta'}_h$ is the Reynolds-averaged heat flux at the top of the CBL due to entrainment. Additionally, the potential temperature profile in the free troposphere is described by

$$\theta_{FT} = \langle\theta\rangle_0 + \Delta\theta_0 + \gamma_\theta (z - h_0). \tag{4}$$

A common closure assumption (Stull 1988) to solve the set of three governing equations with four unknown variables $\left(h, \langle\theta\rangle, \Delta\theta, \overline{w'\theta'_h}\right)$ is to relate the entrainment heat flux at the top of the CBL to the surface flux by

$$\overline{w'\theta'}_h = -\beta\overline{w'\theta'}_0, \tag{5}$$

where β is the entrainment constant, where we usually assume $\beta = 0.2$. Equation 2 then becomes

$$\frac{d\langle\theta\rangle}{dt} = (1 + \beta)\frac{\overline{w'\theta'}_0}{h}. \tag{6}$$

The adaptation of these governing equations to include moisture will be discussed in Sect. 2.3.

2.2 Analytical Solutions

First, we discuss the dependencies of the boundary-layer averaged potential temperature, $\langle\theta\rangle$, and the potential temperature jump at the inversion, $\Delta\theta$, on the boundary-layer height, which are derived in Appendix A1. Second, these relations are used to derive the expression for the boundary-layer height evolution in Appendix A2. It is important to note that we include all the terms without assumptions about the initial conditions of Eqs. 1–3 to obtain the analytical solution presented below, as opposed to previous solutions presented in the literature (e.g., Betts 1973; Garratt 1992; Porporato 2009). As shown by Eq. 64,

$$\Delta\theta = \frac{\beta}{1+2\beta}\gamma_\theta h + \left(\Delta\theta_0 h_0^{\frac{1+\beta}{\beta}} - \frac{\beta}{1+2\beta}\gamma_\theta h_0^{\frac{1+2\beta}{\beta}}\right) h^{-\frac{1+\beta}{\beta}}. \tag{7}$$

A set of assumptions that, with the exception of Driedonks (1982), is commonly made in the analysis of the temporal evolutions in the ABL, results in ignoring the non-linear dependence of the potential temperature jump at the inversion on the boundary-layer height, i.e. the second term on the right-hand site (r.h.s.) in Eq. 7. This restricts the resulting solutions to be valid only for idealized situations. One of these assumptions is a priori considering that the ratio of the potential temperature jump over the boundary-layer height is fixed. In that case, Eq. 50 becomes $\Delta\theta = \left(\frac{\beta}{1+2\beta}\right)\gamma_\theta h$ (Betts 1973; Garratt 1992). Another assumption is stating as an initial condition that h and $\Delta\theta$ are both zero (e.g., Porporato 2009), resulting in $c_3 = 0$ in Eq. 50 and again resulting in $\Delta\theta = \left(\frac{\beta}{1+2\beta}\right)\gamma_\theta h$. This latter assumption would be valid if every day the boundary layer would start its growth from the Earth's surface ($h_0 = 0$). It therefore omits the morning transition from a nocturnal boundary layer to a daytime boundary layer, which starts with a height, h_0, equal to the nocturnal boundary-layer height.

To study the contribution of the non-linear term to $\Delta\theta$ and its importance, the dependency of $\Delta\theta$ on h is shown for different conditions in Fig. 1. The situation evaluated in Fig. 1a considers $\beta = 0.2$, $\gamma_\theta = 0.007\,\mathrm{K\,m^{-1}}$ and an initial boundary-layer height of $h_0 = 500\,\mathrm{m}$. The three situations correspond to an initial potential temperature jump of 0.25 K, 0.5 K and 0.75 K. Under these conditions, the second term on the r.h.s. of Eq. 7 is zero for $\Delta\theta_0 = 0.5\,\mathrm{K}$ and the potential temperature jump increases linearly with height. For the other two cases, the potential temperature jump gradually moves to the linear profile with increasing boundary-layer height according to the second term on the r.h.s. of Eq. 7. From this expression it follows that, for $\beta = 0.2$, the difference between the actual potential temperature jump and the potential temperature jump from the linear profile decreases with the ABL height according to a h^{-6} function.

Using the classification proposed by Tennekes (1973), three different phases can be distinguished in the figure in case the non-linear contribution to $\Delta\theta(h)$ is significant. Here we focus on the situation with a stronger initial potential temperature jump at the top of the ABL. The three phases are the break-up of the morning inversion, a transitional phase and pure convective growth. During the first phase, the boundary layer grows only very slowly due to the strong inversion that formed during night and most energy due to the surface heating is used to erode this inversion and reach the $\Delta\theta(h)$ that corresponds with the linear approximation. The dependence of $\Delta\theta$ on h is governed by the term $\left(\Delta\theta_0 h_0^{\frac{1+\beta}{\beta}} - \left(\frac{\beta}{1+2\beta}\right)\gamma_\theta h_0^{\frac{1+2\beta}{\beta}}\right) h^{-\frac{1+\beta}{\beta}}$ in Eq. 7, which falls with h^{-6}. Even though this phase only holds for a limited range of h values, depending on the surface heat flux it can last for several hours as the boundary-layer growth is slow. The stronger the initial potential temperature jump, the slower is the initial boundary-layer growth. In the second phase, the evolution of the boundary-layer dynamics and, consequently, $\Delta\theta(h)$ is significantly influenced by both the initial conditions and convective growth. The value of $\Delta\theta$ does not strongly change with h. However, since the convective growth is less limited by the initial conditions, the boundary-layer growth increases strongly and this phase does not last for a long period. In the third and final phase, $\Delta\theta(h)$ has reached the linear profile that is associated with simplified initial conditions. By then the tendencies of the CBL properties are only governed by the convective growth of the boundary layer and not by the initial conditions. Note that this only holds for the tendencies and not for the actual values of the CBL properties themselves. As an example, in a situation that starts with a stronger nocturnal inversion, the final boundary-layer height at the end of the
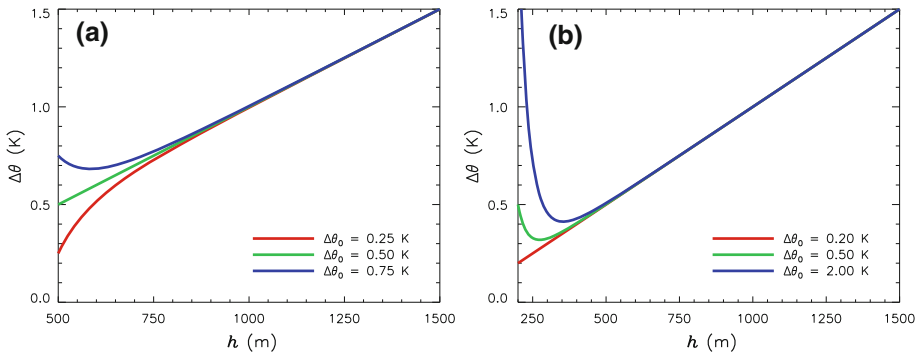
Fig. 1 Dependency of the potential temperature jump on the ABL height for **a** an initial height, h_0, of 500 m, and **b** an initial height of 200 m. For $\Delta\theta_0 = 0.5\,\mathrm{K}$ in **a**, the potential temperature jump increases linearly with the ABL height under the chosen set of initial conditions. In **b**, with its lower initial height, the potential temperature jump only increases linearly with the ABL height for $\Delta\theta_0 = 0.2\,\mathrm{K}$

afternoon will still be lower than in a situation that starts with a weaker nocturnal inversion. At the start of this third phase, the boundary layer grows more rapidly, since the morning inversion no longer influences the entrainment velocity. However, as time progresses and the boundary layer becomes deeper, keeping $\Delta\theta$ small enough when the ABL grows requires relatively more energy. Consequently, the rate of growth of the ABL decreases with increasing boundary-layer height. As the final boundary-layer height is lower and the heat fluxes are unaltered, the final mixed-layer averaged θ is larger.

The evolution of $\Delta\theta$ is dominated by the second term on the r.h.s. of Eq. 7 in the first phase and by the first term on the r.h.s. of Eq. 7 in the third phase. From Eq. 7 we derive

$$\frac{\mathrm{d}\Delta\theta}{\mathrm{d}h} = Grad_{Conv} + Grad_{IC}, \tag{8}$$

$$Grad_{Conv} = \frac{\beta}{1+2\beta}\gamma_\theta, \tag{9}$$

$$Grad_{IC} = -\frac{1+\beta}{\beta}\left(\Delta\theta_0 h_0^{\frac{1+\beta}{\beta}} - \frac{\beta}{1+2\beta}\gamma_\theta h_0^{\frac{1+2\beta}{\beta}}\right) h^{-\frac{1+2\beta}{\beta}}, \tag{10}$$

where $Grad_{IC}$ is the evolution of $\Delta\theta$ due to the initial conditions and $Grad_{Conv}$ is the evolution of $\Delta\theta$ due to convective growth. In the first phase, $|Grad_{Conv}| \gg |Grad_{IC}|$ and in the third phase $|Grad_{Conv}| \ll |Grad_{IC}|$. The exact timing of the transition between two phases is arbitrary. Here, the criterion we use for a phase is that the one contribution is X times as strong as the other. In that case it follows from Eqs. 9 and 10 that

$$h < \left(\frac{1}{X}\frac{\left|\Delta\theta_0 h_0^{\frac{1+\beta}{\beta}} - \left(\frac{\beta}{1+2\beta}\right)\gamma_\theta h_0^{\frac{1+2\beta}{\beta}}\right|}{\gamma_\theta}\frac{1+3\beta+2\beta^2}{\beta^2}\right)^{\frac{\beta}{1+2\beta}} \quad \text{for phase 1,} \tag{11}$$

$$h > \left(X\frac{\left|\Delta\theta_0 h_0^{\frac{1+\beta}{\beta}} - \left(\frac{\beta}{1+2\beta}\right)\gamma_\theta h_0^{\frac{1+2\beta}{\beta}}\right|}{\gamma_\theta}\frac{1+3\beta+2\beta^2}{\beta^2}\right)^{\frac{\beta}{1+2\beta}} \quad \text{for phase 3.} \tag{12}$$

For the examples of Fig. 1, when taking $X = 2$, the transition from phase 1 to phase 2 is at $h = 530$ m and 320 m for Fig. 1a, b, respectively. The transition from phase 2 to phase 3 for these values is at $h = 646$ m and 390 m, respectively. These ABL heights can be related to the elapsed time by using Eq. 94 if the time evolutions of the surface fluxes are known.

After discussing the influence of $\Delta\theta_0$ for situations in which $h_0 = 500$ m, the influence of h_0 itself is explored. In Fig. 1b a case with a more prominent nocturnal inversion is shown. Over land, nocturnal boundary layers with even larger potential temperature jumps, of the order of several K, can occur due to e.g. advection of air masses (Vilà-Guerau de Arellano 2007). As the nocturnal boundary-layer growth is inhibited increasingly by stronger inversions (Garratt 1992), the final nocturnal boundary-layer height will be lower as well. Therefore, for these situations the initial boundary-layer height for the CBL of the consecutive day will be lower and the initial potential temperature inversion of the CBL will be stronger than for more moderate nocturnal inversions. For the situations in Fig. 1b, h_0 is set equal to 200 m and the initial potential temperature jumps are 0.2 K, 0.5 K and 2 K. For an initial boundary-layer height this low $\Delta\theta_0$ of a few K is common, while 0.2 K is the initial potential temperature inversion that corresponds to the linear approximation of $\Delta\theta = \left(\frac{\beta}{1+2\beta}\right)\gamma_\theta h$. The figure shows that, therefore, the effect of the initial conditions on $\Delta\theta(h)$ become more significant for the lower boundary-layer heights. As a consequence, the three aforementioned regimes are more easily recognizable in Fig. 1b compared to Fig. 1a. Since the non-linear part of Eq. 7 can be written as $\left(\Delta\theta_0 - \left(\frac{\beta}{1+2\beta}\right)\gamma_\theta h_0\right)\left(\frac{h}{h_0}\right)^{-\frac{1+\beta}{\beta}}$ and h_0 is smaller, its influence is significant for lower values of h compared to situations with larger h_0. On the other hand, the accompanying stronger $\Delta\theta_0$ inhibits the boundary-layer growth to a greater degree, so that the boundary layer remains shallow for a longer period. In total, also for lower h_0 the initial conditions are significant for the evolution of the boundary-layer dynamics.

Using the knowledge of $\Delta\theta(h)$ and $\theta_{FT}(h)$, i.e. the potential temperature at the bottom of the free troposphere, Eq. 66 is derived. This expression for $\langle\theta\rangle(h)$ reads

$$\langle\theta\rangle = \langle\theta\rangle_0 - \gamma_\theta h_0 + \Delta\theta_0 + \left(\frac{1+\beta}{1+2\beta}\right)\gamma_\theta h - \left(\Delta\theta_0 h_0^{\frac{1+\beta}{\beta}} - \left(\frac{\beta}{1+2\beta}\right)\gamma_\theta h_0^{\frac{1+2\beta}{\beta}}\right)h^{-\frac{1+\beta}{\beta}}. \tag{13}$$

Note that, for relatively large h (larger than ± 750 m for the conditions of Fig. 1), if all other initial conditions are kept the same, $\langle\theta\rangle(h)$ is a linear function whose offset depends on the initial potential temperature jump. This agrees with Fig. 1, since for large h, $\Delta\theta(h)$ becomes independent of the initial conditions. According to Eq. 4, $\theta_{FT}(h)$ is offset by differences in $\Delta\theta_0$ and, consequently, so is $\langle\theta\rangle(h)$ for large h. This relationship is demonstrated in Fig. 2 for the same conditions as Fig. 1a.

As an expression for $\Delta\theta\frac{dh}{dt}$ is known from Eq. 48 and $\Delta\theta(h)$ is provided by Eq. 7, a differential equation for h is found that is independent of $\Delta\theta$ and $\langle\theta\rangle$. The result, given by Eq. 70, is

$$h^2 - \left(\frac{2+4\beta}{\gamma_\theta}\right)\left(\Delta\theta_0 h_0^{\frac{1+\beta}{\beta}} - \left(\frac{\beta}{1+2\beta}\right)\gamma_\theta h_0^{\frac{1+2\beta}{\beta}}\right)h^{-\frac{1}{\beta}}$$

$$= h_0^2 - \left(\frac{2+4\beta}{\gamma_\theta}\right)\left(\Delta\theta_0 h_0 - \left(\frac{\beta}{1+2\beta}\right)\gamma_\theta h_0^2\right) + \left(\frac{2+4\beta}{\gamma_\theta}\right)\int_{t_0}^{t}\overline{w'\theta'}_0 dt. \tag{14}$$

Fig. 2 Dependency of the mixed-layer averaged potential temperature on the ABL height. For $\Delta\theta_0 = 0.5$ K, the potential temperature increases linearly with the ABL height under the chosen set of initial conditions. For other $\Delta\theta_0$, $\langle\theta\rangle(h)$ approaches with increasing h a linear asymptote that does not cross the initial conditions, but is offset by the difference in $\Delta\theta_0$
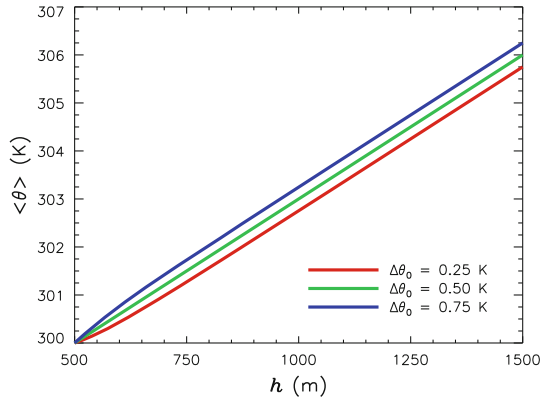
This solution is implicit and cannot be solved explicitly for general values of β. However, for relatively large h, the second term on the left-hand side (l.h.s.) becomes small and can be ignored. This results in the explicit approximation of Eq. (73),

$$
h \approx \sqrt{\underbrace{h_0^2 - \left(\frac{2+4\beta}{\gamma_\theta}\right)\left(\Delta\theta_0 h_0 - \left(\frac{\beta}{1+2\beta}\right)\gamma_\theta h_0^2\right)}_{-\frac{2+4\beta}{\gamma_\theta}D_0} + \left(\frac{2+4\beta}{\gamma_\theta}\right)\int_{t_0}^{t}\overline{w'\theta'}_0 \mathrm{d}t}. \quad (15)
$$

Equation 15 matches the equations previously presented by Driedonks (1982). Apart from notation, the only small difference the reader might note, is found in the second term on the l.h.s. of the implicit solution (Eq. 8 in his manuscript) where a multiplication with β is omitted. The sum of the first two terms in the square root is identified as $-\frac{2+4\beta}{\gamma_\theta}$ times the initial temperature deficit, D_0. This initial temperature deficit describes how much heat is needed to fill the nocturnal inversion that is present at the start of the day. Note that Eq. 15 confirms that, for $h \gg h_0$, even though $\Delta\theta(h)$ is unaffected by the initial conditions, $h(t)$ and, consequently, $\Delta\theta(t)$ remain affected by the initial temperature deficit during the entire day. The explicit approximation of Eq. 15 is evaluated in more detail in Sect. 3.

From Eqs. 7, 13, 14 and 15 it is clear that for the chosen conditions the evolutions $h(t)$, $\langle\theta\rangle(t)$ and $\Delta\theta(t)$ are only dependent on time through the integrated surface heat flux, $\int_{t_0}^{t}\overline{w'\theta'}_0 \mathrm{d}t$. This is independent of the distribution of the surface heat flux over time and the amount of time needed to reach that value of integrated surface heat flux. This will be confirmed in Sect. 3.3.

2.3 Including the Effects of Moisture

If moisture is present, the specific humidity, q, has to be accounted for in the expression of the boundary-layer height evolution. The variable that drives convection is then the virtual potential temperature, θ_v, instead of the potential temperature. This virtual potential temperature and its transport are expressed by (Stull 1988)

$$
\theta_v = \theta\left(1 + 0.61q\right), \quad (16)
$$

$$
\overline{w'\theta'_v} \approx 0.61\,\overline{\theta}\,\overline{w'q'} + (1 + 0.61\,\overline{q})\,\overline{w'\theta'}. \quad (17)
$$

The closure assumption of Eq. 5 is altered to

$$\overline{w'\theta'_v}_h = -\beta\overline{w'\theta'_v}_0. \tag{18}$$

As shown in Appendix A4, the new governing equations are derived by assuming a vertical profile of the specific humidity that, just like the potential temperature, is constant in the boundary layer, has a discontinuity at the inversion and is linear in the free troposphere. In contrast to the case without moisture, two approximations have to be used before obtaining the expressions. To justify these approximations, typical values for variables in the CBL will be applied. The first approximation holds that $|\Delta\theta\Delta q| \ll \Delta\theta_v$, considering that q in these equations should be expressed in the dimensionless $\mathrm{kg\,kg^{-1}}$. For the clear boundary layer over land, this is valid as $\Delta\theta$ is of similar magnitude as $\Delta\theta_v$, and Δq is of the order of $10^{-3}\,\mathrm{kg\,kg^{-1}}$.

The second approximation is to consider the virtual potential temperature lapse rate in the free troposphere, $\gamma_{\theta_v} = \frac{d\theta_v}{dz}$, to be constant with height, while actually

$$\gamma_{\theta_v}(z) = (1 + 0.61q(z))\,\gamma_\theta + 0.61\theta(z)\gamma_q. \tag{19}$$

The approximation that is applied considers $\gamma_{\theta_v}(z) \approx \gamma_{\theta_v}(h_0)$. For the first term in Eq. 19, $0.61q(z)$ is of the order of $10^{-3}\,\mathrm{kg\,kg^{-1}}$, so that

$$1 + 0.61q(h_0) \approx 1 + 0.61q(z)$$

for all heights considered when evaluating the atmospheric boundary layer. For the second term, $\theta \approx 300$ K and γ_q describes changes in specific humidity with height, which are of the order of $\mathrm{g\,kg^{-1}\,km^{-1}}$. This results in a contribution to γ_{θ_v} of the order of $10^{-1}\,\mathrm{K\,km^{-1}}$, which can be significant. However, for an evolving CBL the change in $\theta(z)$ just above the mixed layer is only of the order of 10 K. Because of that, using $\theta(h_0)$ instead of $\theta(z)$ results in a change in γ_{θ_v} of the order of $10^{-2}\,\mathrm{K\,km^{-1}}$. Therefore,

$$0.61\,(\theta(z) - \theta(h_0))\,\gamma_q \ll \gamma_\theta.$$

As an example to show that we can indeed assume γ_{θ_v} to be constant, consider the situation described in Table 1 that includes moisture. We consider γ_q to be $\pm 0.001\,\mathrm{g\,kg^{-1}\,m^{-1}}$. We compare γ_{θ_v} and θ_v at 2,000 m height as calculated with the approximation and as calculated with the prescribed θ and q profiles. For $\gamma_q = 0.001$ g $\mathrm{kg^{-1}\,m^{-1}}$, the true γ_{θ_v} at 2,000 m height is 0.18 % larger than the approximated value of $6.2 \times 10^{-3}\,\mathrm{K\,m^{-1}}$, which is a difference of $1.1 \times 10^{-5}\,\mathrm{K\,m^{-1}}$. The change has the same magnitude but negative sign if $\gamma_q = -0.001$ g $\mathrm{kg^{-1}\,m^{-1}}$. Finally, θ_v at 2,000 m only differs by 8.2×10^{-3} K.

The resulting set of governing equations that replaces Eqs. 1–3 becomes

$$\frac{dh}{dt} = -\frac{\overline{w'\theta'_v}_h}{\Delta\theta_v}, \tag{20}$$

$$\frac{d\langle\theta_v\rangle}{dt} = \frac{\overline{w'\theta'_v}_0 - \overline{w'\theta'_v}_h}{h}, \tag{21}$$

$$\frac{d\Delta\theta_v}{dt} = \gamma_{\theta_v}\frac{dh}{dt} - \frac{d\langle\theta_v\rangle}{dt}. \tag{22}$$

Property	Without moisture	With moisture
h_0 (m)	500	500
$\langle\theta\rangle_0$ (K)	290	290
$\Delta\theta_0$ (K)	1.5	1.5
γ_θ (K m^{-1})	0.006	0.006
$\overline{w'\theta'}_0$ (K m s^{-1})	0.1	0.1
$\langle q\rangle_0$ (g kg^{-1})	0	6
Δq_0 (g kg^{-1})	0	-2
γ_q (g kg^{-1} m^{-1})	0	0
$\overline{w'q'}_0$ (g kg^{-1} m s^{-1})	0.0	0.1
β	0.2	0.2

Table 1 Initial and boundary conditions that are used for the comparison of the different boundary-layer height expressions in Fig. 3

For this evaluation, the surface fluxes are kept constant with time, disregarding diurnal variability

The surface flux, $\overline{w'\theta'}_{v0}$, is again considered to be prescribed. These relations show that to include moisture, the equations of Sect. 2.2 can be used by replacing θ by θ_v. Therefore

$$
h^2 - \left(\frac{2+4\beta}{\gamma_{\theta_v}}\right)\left(\Delta\theta_{v,0}h_0^{\frac{1+\beta}{\beta}} - \left(\frac{\beta}{1+2\beta}\right)\gamma_{\theta_v}h_0^{\frac{1+2\beta}{\beta}}\right)h^{-\frac{1}{\beta}}
$$

$$
= h_0^2 - \left(\frac{2+4\beta}{\gamma_{\theta_v}}\right)\left(\Delta\theta_{v,0}h_0 - \left(\frac{\beta}{1+2\beta}\right)\gamma_{\theta_v}h_0^2\right) + \left(\frac{2+4\beta}{\gamma_{\theta_v}}\right)\int_{t_0}^{t}\overline{w'\theta'}_{v0}\mathrm{d}t, \quad (23)
$$

which is approximated as

$$
h \approx \sqrt{h_0^2 - \left(\frac{2+4\beta}{\gamma_{\theta_v}}\right)\left(\Delta\theta_{v,0}h_0 - \left(\frac{\beta}{1+2\beta}\right)\gamma_{\theta_v}h_0^2\right) + \left(\frac{2+4\beta}{\gamma_{\theta_v}}\right)\int_{t_0}^{t}\overline{w'\theta'}_{v0}\mathrm{d}t}. \quad (24)
$$

As shown in this section, the approximations that were made to derive this result only lead to insignificant changes. Analogous to Eq. 15, the sum of the first two terms in the square root of Eq. 24, $h_0^2 - \left(\frac{2+4\beta}{\gamma_{\theta_v}}\right)\left(\Delta\theta_{v,0}h_0 - \left(\frac{\beta}{1+2\beta}\right)\gamma_{\theta_v}h_0^2\right)$, describes how much buoyancy needs to be added by the surface buoyancy flux to fill the initial excess inversion in the virtual potential temperature profile.

As before, the evolutions of $h(t)$, $\langle\theta_v\rangle(t)$ and $\Delta\theta_v(t)$ are only dependent on time through the integrated surface buoyancy flux, $\int_{t_0}^{t}\overline{w'\theta'}_{v0}\mathrm{d}t$. As a result, if two different cases have the same initial conditions and time-integrated surface buoyancy flux at certain points in time, the values of h, $\langle\theta_v\rangle$ and $\Delta\theta_v$ at those times are equal as well. For evaluating cases it is important to note that equipment that measures the sensible and latent heat fluxes can return the buoyancy flux as well.

If $h(t)$ is known, the individual time evolutions $\langle\theta\rangle(t)$ and $\langle q\rangle(t)$, and consequently $\Delta\theta(t)$ and $\Delta q(t)$, can be determined if additionally the corresponding surface fluxes are known. This will be treated in Sect. 2.4.

By defining the dimensionless groups

$$\hat{H} = \frac{h}{h_0}, \tag{25}$$

$$\hat{J} = \frac{\Delta\theta_{v,0}}{\gamma_{\theta_v} h_0}, \tag{26}$$

$$\hat{F} = \frac{\int_{t_0}^{t} \overline{w'\theta'_v}_0 \mathrm{d}t}{\gamma_{\theta_v} h_0^2}, \tag{27}$$

Equations 23 and 24 can be written in the dimensionless forms

$$\hat{H}^2 - 2\left((1+2\beta)\hat{J} - \beta\right)\hat{H}^{-\frac{1}{\beta}} = 1 - 2\left((1+2\beta)\hat{J} - \beta\right) + 2(1+2\beta)\hat{F}, \tag{28}$$

$$\hat{H} \approx \sqrt{1 - 2\left((1+2\beta)\hat{J} - \beta\right) + 2(1+2\beta)\hat{F}}, \tag{29}$$

$$\hat{H} \approx \sqrt{1+2\beta}\sqrt{1 + 2\left(\hat{F} - \hat{J}\right)}. \tag{30}$$

$\hat{H}$ is related to the boundary-layer height compared to its initial value, $\hat{J}$ expresses the relative strength of the initial virtual potential temperature jump at the inversion and $\hat{F}$ denotes the scaled time-integrated surface buoyancy flux. Equation 30 shows that for relatively large $\hat{H}$ the growth of the boundary layer is governed by the difference between the scaled time-integrated surface buoyancy flux and the relative strength of the initial virtual potential temperature jump compared to the free tropospheric virtual potential temperature profile. Equations 29 and 30 are valid for a large range of $\hat{H}$, as already for e.g. $\hat{H} = 2$ in Eq. 28, $\hat{H}^2 = 128\hat{H}^{-\frac{1}{\beta}}$ if $\beta = 0.2$.

2.4 Evolution of Conserved Scalars

Appendix A3 demonstrates that, as long as an arbitrary scalar, ϕ, is conserved, has no significant additional sources/sinks in the boundary layer (e.g., radiation divergence, phase changes or chemical production/loss), is not horizontally advected or influenced by subsidence, and has a vertical profile in the free troposphere that is characterized by a constant gradient, γ_ϕ, the evolution of the boundary-layer averaged scalar, $\langle\phi\rangle$, can be expressed as a function of time, the current boundary-layer height and the integral of the emissions after the initial conditions. As the current boundary-layer height, $h(t)$, can be calculated with Eq. 23 or approximated using Eq. 24, only knowledge about the initial conditions and the evolutions of the surface buoyancy flux and scalar emission/deposition are needed to know $\langle\phi\rangle(t)$. According to Eq. 76,

$$\langle\phi\rangle(t) = \langle\phi\rangle_0 + \frac{h(t) - h_0}{h(t)}\Delta\phi_0 + \frac{\gamma_\phi}{2}\frac{(h(t) - h_0)^2}{h(t)} + \frac{1}{h(t)}\int_{t_0}^{t}\overline{w'\phi'}_0\mathrm{d}t. \tag{31}$$

If the scalar under consideration is chemically active, there is additional production or loss and this equation does not hold. However, in idealized conditions the chemical production, P, is constant with time and height. If the chemical reactions that deplete the chemical species are of the first-order with respect to that species, the chemical loss, L, scales linearly with the mixing ratio under consideration. L is then expressed by

$$L = -\frac{\langle\phi\rangle}{\tau}, \tag{32}$$

where τ is the lifetime of the chemical species. The governing equation for $\langle\phi\rangle$ becomes

$$\frac{d\langle\phi\rangle}{dt} = \frac{\overline{w'\phi'}_0 - \overline{w'\phi'}_h}{h} + P - \frac{\langle\phi\rangle}{\tau} \tag{33}$$

and it can be shown that

$$\langle\phi\rangle(t) = \langle\phi\rangle_0\, e^{\frac{t_0-t}{\tau}} + \frac{h(t)-h_0}{h(t)}\Delta\phi_0\, e^{\frac{t_0-t}{\tau}} + \frac{\gamma_\phi}{2}\frac{(h(t)-h_0)^2}{h(t)}e^{\frac{t_0-t}{\tau}}$$

$$+P\tau\left(1 - e^{\frac{t_0-t}{\tau}}\right) + \frac{1}{h(t)}\int_{t_0}^{t}\overline{w'\phi'}_0\, e^{\frac{t'-t}{\tau}}\,dt'. \tag{34}$$

In this equation, the chemical destruction is introduced by the occurrences of $e^{\frac{t_0-t}{\tau}}$. The factor $e^{\frac{t_0-t}{\tau}}$ in the first three terms on the r.h.s. shows that the initial mixing ratio profile decays with the lifetime τ. If the species is inert, the profile should not decay at all. This is reflected in the equations, since in that case $\tau \to \infty$, which results in $e^{\frac{t_0-t}{\tau}} \approx 1 + \frac{t_0-t}{\tau} \approx 1$. Therefore, for $\tau \to \infty$, the first three terms on the r.h.s. in Eq. 34 are equal to the first three terms on the r.h.s. in Eq. 31. For highly reactive chemical species, τ is small and in a short time, e.g. seconds for the hydroxyl radical, $e^{\frac{t_0-t}{\tau}}$ approaches zero. In that case, the initial conditions are not important for the time evolution of the mixing ratio.

The fourth term on the r.h.s. of Eq. 34 describes an equilibrium between chemical production and destruction. If there is no production, $P = 0$ and this term disappears. If not much time has elapsed relative to the chemical lifetime, i.e. $t - t_0 \ll \tau$, then $\tau\left(1 - e^{\frac{t_0-t}{\tau}}\right) \approx \tau - \tau\left(1 + \frac{t_0-t}{\tau}\right) = t - t_0$. In these situations the chemical contribution results in a linear increase in time of the mixing ratio, according to $P(t - t_0)$. For inert chemical species, $\tau \to \infty$ and this always holds true.

For chemical species that do not have an extremely short or long lifetime, this balance between chemical production and destruction first increases linearly with time. When $t - t_0$ becomes of the same order as τ, the rate of increase starts to decrease. Finally, for $t - t_0 \gg \tau$ the balance between chemical production and chemical destruction reaches an asymptote. At that moment, $e^{\frac{t_0-t}{\tau}} \approx 1 + \frac{t_0-t}{\tau} \approx 1$ and thus $P\tau\left(1 - e^{\frac{t_0-t}{\tau}}\right) \approx P\tau$. This shows that the chemical balance results in a mixing ratio that is equal to the chemical production rate times the lifetime of the chemical species.

The final term on the r.h.s. of Eq. 34 expresses the influence of the surface exchange (emission or deposition) on the mixing ratio. Greater boundary-layer heights result in a weaker impact of this term. Due to chemical destruction, emissions that took place a longer time ago have less impact on the current mixing ratio than recent emissions. This is quantified by the factor $e^{\frac{t'-t}{\tau}}$ in the integral.

3 Evaluation

3.1 Accuracy of the Explicit Approximation

The explicit expression of Eq. 24 is a simplification of Eq. 23 by neglecting its second term on the l.h.s. As this term falls with $h^{\frac{-1}{\beta}}$, the explicit approximation is valid for relatively large h, but not for relatively small h. For instance, at $t = t_0$ the resulting h is expressed by

$$h = \sqrt{h_0^2 - \left(\frac{2+4\beta}{\gamma_{\theta_v}}\right)\left(\Delta\theta_{v,0}h_0 - \left(\frac{\beta}{1+2\beta}\right)\gamma_{\theta_v}h_0^2\right)} \tag{35}$$

instead of $h = h_0$. The difference between the explicit approximation and the real boundary-layer height, as obtained from the implicit expression, becomes smaller for increasing h. An analysis of the l.h.s. of Eq. 23 shows that the accuracy of the explicit solution,

$$\alpha = \frac{\left|h_{\text{explicit}} - h_{\text{implicit}}\right|}{h_{\text{implicit}}}, \tag{36}$$

is related to the boundary-layer height in such a way that the height can be found for which a certain accuracy is obtained. The explicit simplification of the boundary-layer height is within a certain accuracy of the true (implicitly determined) boundary-layer height if

$$\begin{cases} h(\alpha) \geq (1-\alpha)\left(\left(\frac{2+4\beta}{\gamma_{\theta_v}}\right)\frac{\Delta\theta_{v,0}h_0^{\frac{1+\beta}{\beta}} - \left(\frac{\beta}{1+2\beta}\right)\gamma_{\theta_v}h_0^{\frac{1+2\beta}{\beta}}}{\alpha(2-\alpha)}\right)^{\frac{\beta}{1+2\beta}} & \text{if } \Delta\theta_{v,0} > \left(\frac{\beta}{1+2\beta}\right)\gamma_{\theta_v}h_0, \\[4mm] h(\alpha) \geq (1+\alpha)\left(\left(\frac{2+4\beta}{\gamma_{\theta_v}}\right)\frac{\left(\frac{\beta}{1+2\beta}\right)\gamma_{\theta_v}h_0^{\frac{1+2\beta}{\beta}} - \Delta\theta_{v,0}h_0^{\frac{1+\beta}{\beta}}}{\alpha(2+\alpha)}\right)^{\frac{\beta}{1+2\beta}} & \text{if } \Delta\theta_{v,0} < \left(\frac{\beta}{1+2\beta}\right)\gamma_{\theta_v}h_0. \end{cases}$$

Illustrative values are presented for two different situations in Sect. 3.3.

3.2 Hybrid Explicit Expression

The mismatch of Eq. 24 for small h would be removed if the true h were substituted in the second term on the l.h.s. of Eq. 23. Although no perfect explicit solution exists, the previously published boundary-layer height development (Garratt 1992), which assumes $\Delta\theta_v$ to be linearly dependent on h, could be used for this substitution to decrease the mismatch. The expression for this evolution, $\hat{h}$, is

$$\hat{h} = \sqrt{h_0^2 + \left(\frac{2+4\beta}{\gamma_{\theta_v}}\right)\int_{t_0}^{t}\overline{w'\theta'}_{v0}dt} \tag{37}$$

and results in $\hat{h} = h_0$ at $t = t_0$. Furthermore, in reality the typical reason that at the start of the day $\Delta\theta_{v,0} \neq \left(\frac{\beta}{1+2\beta}\right)\gamma_{\theta_v}h_0$, is the lower potential temperature in the boundary layer compared to the free troposphere due to radiative cooling during the night. This results in $\Delta\theta_{v,0} > \left(\frac{\beta}{1+2\beta}\right)\gamma_{\theta_v}h_0$. From Eq. 23 it can be seen that in that case for $h > h_0$, $h < \sqrt{h_0^2 + \left(\frac{2+4\beta}{\gamma_{\theta_v}}\right)\int_{t_0}^{t}\overline{w'\theta'}_{v0}dt} = \hat{h}$. Therefore, $\hat{h}^{\frac{-1}{\beta}} < h^{\frac{-1}{\beta}}$, which means that by substituting
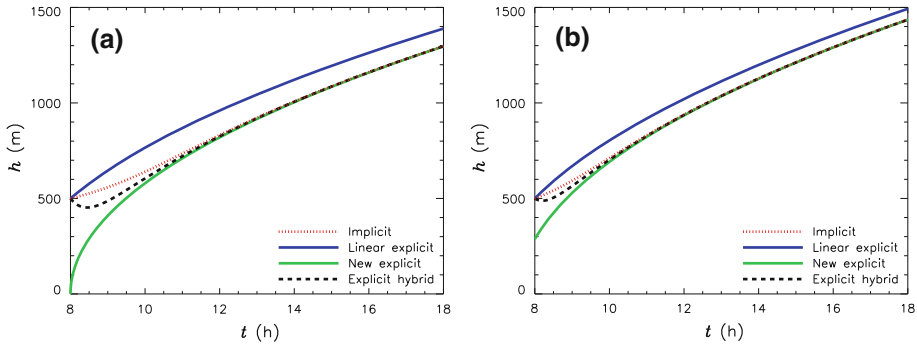
Fig. 3 Boundary-layer height evolution representations for, **a** a situation without, and **b** a situation with moisture present. Each *panel* shows the implicit solution for h, the old explicit solution that assumes $\Delta\theta$ to be linearly dependent on h and the new explicit simplification, which ignores the second term of the l.h.s. of the implicit expression (Eq. 23). This term falls with $h^{\frac{-1}{\beta}}$. Finally, the *black line* shows the hybrid explicit solution, which is obtained by substituting the linear explicit solution into the h of the aforementioned term of Eq. 23

$\hat{h}$ in the second term of Eq. 23, this term is no longer put to zero, but its magnitude will still be less than if the true h were used. The resulting hybrid explicit expression for the boundary-layer height is

$$h_{\text{hybrid}} = \left[h_0^2 + \left(\frac{2+4\beta}{\gamma_{\theta_v}}\right)\left(\Delta\theta_{v,0}h_0^{\frac{1+\beta}{\beta}} - \left(\frac{\beta}{1+2\beta}\right)\gamma_{\theta_v}h_0^{\frac{1+2\beta}{\beta}}\right)\left(\hat{h}^{-\frac{1}{\beta}} - h_0^{-\frac{1}{\beta}}\right) \right.$$
$$\left. + \left(\frac{2+4\beta}{\gamma_{\theta_v}}\right)\int_{t_0}^{t}\overline{w'\theta'_{v0}}\,\mathrm{d}t \right]^{1/2}. \tag{38}$$

For practical everyday use, we propose to use this representation of h if $\Delta\theta_{v,0} \geq \left(\frac{\beta}{1+2\beta}\right)\gamma_{\theta_v}h_0$, as it captures the evolution of h for both relatively small and relatively large h. A comparison between the different expressions for h is discussed in Sect. 3.3.

3.3 Comparison Between Solutions

In this section, four different representations of the boundary-layer height are compared: the *implicit*, *linear explicit*, *new explicit* and *explicit hybrid* solution. The *implicit* expression describes the exact boundary-layer height evolution, which is equal to the one that results from numerically solving Eqs. 20–22. This equivalence is tested for multiple situations (not shown) by comparing the l.h.s. of Eq. 23 to the corresponding output of a numerical mixed-layer model. Since the results were equal and the l.h.s. of Eq. 23 is bijective with h (Appendix A5), the corresponding evolutions of h are equal as well. The *linear explicit* expression is the common solution for the boundary-layer height that assumes $\Delta\theta_v$ to be linearly dependent on h (e.g., Garratt 1992). The *new explicit* expression is Eq. 24, which takes all initial conditions into account. Note that, due to being a simplification of the *implicit* expression, the initial state for the *new explicit* expression is not equal to the initial conditions (see Eq. 35). Finally, the *explicit hybrid* expression is the combined explicit approximation that is derived in Sect. 3.2.

Fig. 4 Evolution of $\langle q \rangle$ as calculated by Eq. 31 using the different expressions for the boundary-layer height evolution that are shown in Fig. 3b. These expressions are the implicit solution for h, the old explicit solution that assumes $\Delta \theta$ to be linearly dependent on h and the new explicit simplification. Finally, the *black line* shows the evolution if the hybrid explicit solution for h is used
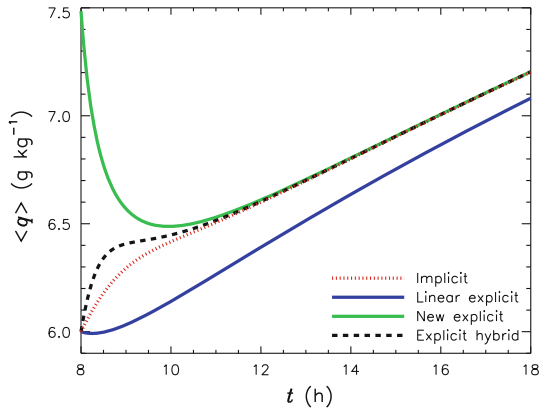
All four representations are presented in Fig. 3 for a boundary layer with an initial height of 500 m. Two situations are considered: one without and one with moisture present. The initial and boundary conditions are presented in Table 1.

The figures show the importance of the non-linear term of $\Delta \theta_v$ in reproducing the evolution of the ABL height. The difference after 10 h between the *linear explicit* representation and the true boundary-layer height is 90 m for the case without moisture and 60 m for the case with moisture. The *new explicit* expression of Eq. 24 performs poorly in the initial stage. However, it matches the implicit height better with increasing h. The new expression already performs better than the linear expression for $h = 600$ m and is indistinguishable from the implicit solution for $h = 700$ m. According to the relations of Sect. 3.1, the differences with the true boundary-layer height for the dry and the moist situation are 5 % at 662 m and 626 m, respectively, and only 1 % at 866 m and 818 m, respectively. Finally, Fig. 3 shows that the hybrid explicit expression for the boundary-layer height of Eq. 38 does approximate the implicit representation of the boundary-layer height best. It retains the accurate representativeness of the new explicit expression for large h and solves the initial mismatch. Note that the *hybrid* expression only significantly improves on the *new explicit* expression if the *linear explicit* expression returns a boundary-layer height similar to the actual boundary-layer height. If the height according to the *new explicit* expression is much higher, $\hat{h}^{-\frac{1}{\beta}}$ in Eq. 38 becomes too insignificant and the *hybrid* solution will become similar to the *new explicit* expression. This occurs for strong initial potential temperature jumps.

As expressed by Eq. 31, the evolution of the scalars in the boundary layer depends on the ABL height evolution. To show the relevance of an accurate expression, Fig. 4 presents the diurnal evolution of $\langle q \rangle$ for the situation with moisture from Table 1. The four different lines are the evolutions that result from substituting the four different boundary-layer height evolutions of Fig. 3b in Eq. 31. Substituting the *implicit* expression for h results in the true expression of $\langle q \rangle (t)$. The evolution of $\langle q \rangle$ that is based on the explicit *hybrid* expression for h is more accurate than that calculated with the original *linear explicit* expression. After 1 hour of simulated time, using the *new explicit* expression, which is accurate for large h, results in a better representation of the evolution of $\langle q \rangle$ than using the original *linear explicit* expression as well. Near the end of the day, the value of $\langle q \rangle$ as obtained by the *linear explicit* expression is an underestimation of 0.12 g kg^{-1}, which is 10 % of the total increase in $\langle q \rangle$ during the day, 1.2 g kg^{-1}. This underestimation can significantly affect ABL representations
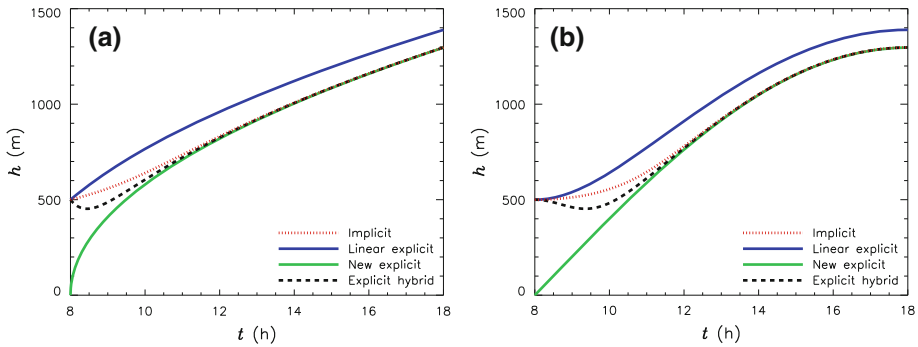
Fig. 5 Boundary-layer height evolution representations for, **a** a constant, and **b** a sinus-shaped surface heat flux. Each *panel* shows the implicit solution for h, the old explicit solution that assumes $\Delta\theta$ to be linearly dependent on h and the new explicit simplification, which ignores the second term of the l.h.s. of the implicit expression (Eq. 23). This term falls with $h^{\frac{-1}{\beta}}$. Finally, the *black line* shows the hybrid explicit solution, which is obtained by substituting the linear explicit solution into the h of the aforementioned term of Eq. 23

(Vilà-Guerau de Arellano 2007), e.g. by inaccurately predicting the timing of saturation at the top of the boundary layer and the subsequent formation of clouds.

To predict the final boundary-layer height using the different expressions, only the integrated value of the surface heat flux is of importance and not its specific distribution over the day. This is shown in Fig. 5. In Fig. 5a, the situation without moisture from Table 1 is repeated. In Fig. 5b, this case is adapted to consider a more realistic, sinus-shaped evolution of the surface heat flux. For fair comparison the maximum value of this sinus is selected such that over the 10 h of simulation, the integrated surface heat flux is equal to the original situation. To this end, we prescribe a surface heat flux of

$$\overline{w'\theta'}_{0,\text{Sine}}(t) = \frac{\pi}{2}\overline{w'\theta'}_0 \sin\left(\frac{\pi t}{T}\right), \tag{39}$$

where t is the elapsed time since the start of the simulation and T is the simulated period, both of which should be expressed in the same units. Due to the different distributions in time of the surface heat flux, the timing of the boundary-layer height evolution changed, but the final boundary-layer properties are identical. Because of the low heat fluxes at the start and at the end of the day, the ABL growth is much slower in these phases, resulting in more curved shapes for the boundary-layer height evolutions.

3.4 Sensitivity of h

An advantage of having the analytical solution for h (Eq. 24) is the possibility of studying its sensitivity to different initial and boundary conditions. h depends on five variables: $\beta, \gamma_{\theta_v}, h_0, \Delta\theta_{v,0}$ and I, where I is the time-integrated surface buoyancy flux.

$$I = \int_{t_0}^{t} \overline{w'\theta'_{v0}}\,\mathrm{d}t. \tag{40}$$

Defining the initial virtual temperature deficit, $D_{v,0}$, as

$$D_{v,0} = \Delta\theta_{v,0}h_0 - \frac{1}{2}\gamma_{\theta_v}h_0^2, \tag{41}$$

Table 2 Sensitivity of the boundary-layer height, h, after 10 h of simulation to the different initial and boundary conditions

Property	Sensitivity	Min	Max	Property range (%)	h range (%)
β (–)	0.14	0.1	0.3	100	14
γ_{θ_v} (K m^{-1})	-0.42	$3 \cdot 10^{-3}$	$7 \cdot 10^{-3}$	67	28
I (K m)	0.48	2,975	5,525	60	29
h_0 (m)	0.10	300	700	80	8
$\Delta\theta_{v,0}$ (K)	-0.06	0.15	2.15	174	11

The sensitivity of h to a change in any arbitrary variable, ψ, is expressed as $\left(\frac{\partial h}{h}\right) / \left(\frac{\partial \psi}{\psi}\right)$. The property range expresses for every variable, ψ, the range $\max_\psi - \min_\psi$ as a percentage of the standard value of ψ, which is based on Table 1. The standard values that cannot be read directly from that table are $\gamma_{\theta_v} = 6 \times 10^{-3}$ K m^{-1}, I = 4250 K m and $\Delta\theta_{v,0} = 1.15$ K. The last column presents the resulting relative range in h

squaring Eq. 24 results in

$$h^2 = \frac{2 + 4\beta}{\gamma_{\theta_v}} \left(I - D_{v,0}\right). \tag{42}$$

Similar to previous work by Driedonks (1982) for β, γ_{θ_v} and I, by differentiating this expression to the five different governing variables of Eq. 24 we can derive

$$\frac{\partial h}{h} = \left(\frac{\beta}{1 + 2\beta}\right) \frac{\partial \beta}{\beta} \qquad \text{for } \beta, \tag{43}$$

$$\frac{\partial h}{h} = -\left(\frac{1}{2} - \frac{\gamma_{\theta_v} h0^2}{4\left(I - D_{v,0}\right)}\right) \frac{\partial \gamma_{\theta_v}}{\gamma_{\theta_v}} \quad \text{for } \gamma_{\theta_v}, \tag{44}$$

$$\frac{\partial h}{h} = \frac{I}{2\left(I - D_{v,0}\right)} \frac{\partial I}{I} \qquad \text{for } I, \tag{45}$$

$$\frac{\partial h}{h} = \frac{\gamma_{\theta_v} h_0^2 - \Delta\theta_{v,0} h_0}{2\left(I - D_{v,0}\right)} \frac{\partial h_0}{h_0} \qquad \text{for } h_0, \tag{46}$$

$$\frac{\partial h}{h} = -\frac{\Delta\theta_{v,0} h_0}{2\left(I - D_{v,0}\right)} \frac{\partial \Delta\theta_{v,0}}{\Delta\theta_{v,0}} \qquad \text{for } \Delta\theta_{v,0}. \tag{47}$$

Note that in this analysis one should consider that $D_{v,0}$ is also dependent on $\Delta\theta_{v,0}$, h_0 and γ_{θ_v}. This consideration explains the difference between the presented Eq. 44 and Eq. (16) of Driedonks (1982).

The sensitivity of h to a change in any arbitrary variable, ψ is expressed as $\left(\frac{\partial h}{h}\right) / \left(\frac{\partial \psi}{\psi}\right)$. To evaluate the importance of the different variables, these sensitivities are evaluated for the conditions of Table 1 with moisture. Similar to Driedonks (1982), for each of the five variables a range of possible values is determined, which is expressed as a percentage of the original value from Table 1. By multiplying this range with the sensitivity, the resulting range in h compared to the original value of 1436 m is found. β is assumed to be between 0.1 and 0.3 (Stull 1988) and γ_{θ_v} is estimated to be between 3×10^{-3} and 7×10^{-3} K m^{-1}. The influence of the integrated heat flux is evaluated for a positive or negative change of 30 % (Driedonks 1982). Values for h_0 are considered to be higher than 300 m and lower than 700 m. Finally, $\Delta\theta_{v,0}$ is assumed to deviate at most 1 K compared to the original value. The

Fig. 6 Sensitivity of the final boundary-layer height, h, to different initial and boundary conditions, ψ. The *horizontal axis* denotes the relative change in these conditions compared to the standard case (Table 1 with moisture). The *vertical axis* denotes the resulting relative change in h. *Solid lines* show the true deviations, which are determined using Eq. 24. *Dashed lines* are linearisations based on $\frac{\mathrm{d}h}{\mathrm{d}\psi}$ for the standard case, multiplied by $\Delta\psi$
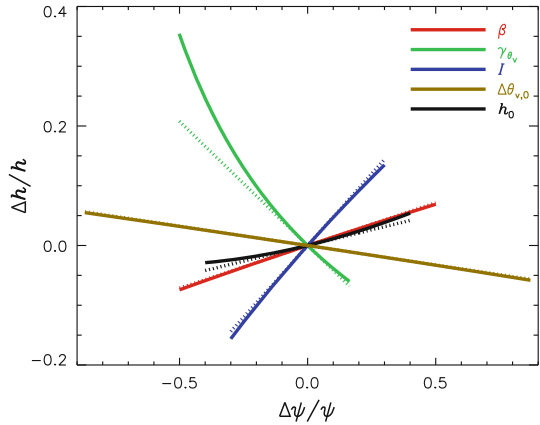
results are summarized in Table 2. This shows that if all variables were to be perturbed by the same percentage, the changes in γ_{θ_v} and I would influence h most with their absolute sensitivities of 42 % and 48 %, respectively. For the chosen typical values, the resulting relative ranges in h are largest for these two variables as well, even though their own relative ranges are smaller than those of the other variables.

Further extending on the sensitivity analysis performed by Driedonks (1982), the calculated sensitivities are presented as dashed lines in Fig. 6. Additionally, the true relative deviations in the boundary-layer height, determined by Eq. 24, are drawn with solid lines. The solid lines deviate from the linear dashed lines, since for all initial and boundary conditions, ψ, the sensitivities are dependent on ψ itself. For example, Eq. 43 shows $\left(\frac{\partial h}{h}\right)\Big/\left(\frac{\partial \beta}{\beta}\right)=\frac{\beta}{1+2\beta}$. However, even for γ_{θ_v}, where this deviation of the solid line from the dashed line is most present, the effect is insignificant as long as the relative deviation in the condition remains <20 %.

To conclude, Fig. 6 displays the application of Eq. 24 to study the response of h to a wide range of initial and boundary conditions by two different methods. For the first method the equation is used to determine a sensitivity to these conditions, which can be used to relate changes in the conditions to changes in the boundary-layer height with a single number. The second method is to plot the solution as a function of these conditions to study the exact response of h for a larger range. The same analyses can be applied to study the sensitivity of other variables, such as $\langle\theta\rangle$, by using Eqs. 31 or 34.

3.5 Subsidence

In this study, cases with large-scale atmospheric subsidence are not considered. The analytical solutions, which were originally derived for a basic situation without subsidence, could not be extended to include this effect. To understand why this is not possible with the currently applied mathematical method, one needs to consider a basic, dry situation with subsidence, a certain boundary-layer height, $h = h_0$, and a certain potential temperature jump, $\Delta\theta = \Delta\theta_0$. In this situation, it can be deduced that $\Delta\theta$ is not only dependent on h, but also on time. If the effect of subsidence can be ignored and the boundary-layer height changes due to entrainment, $\Delta\theta$ changes with height, independent of the time it takes to reach the new height. Therefore, if the changes in the boundary-layer height occur in a very short time period, so that the effects of subsidence are infinitesimally small, in general $\Delta\theta \neq \Delta\theta_0$ if

$h \neq h_0$. However, if the entrainment process is slow compared to subsidence, the boundary-layer height decreases due to the subsidence. During this process, $\Delta\theta$ remains equal to $\Delta\theta_0$ as the subsiding motions do not alter the potential temperatures below and just above the inversion. In this case $\Delta\theta = \Delta\theta_0$ for a certain $h < h_0$. If then (a sudden burst of) entrainment compensates the decrease in the boundary-layer height, the potential temperature jumps again changes, resulting in a different value than $\Delta\theta_0$. Therefore $\Delta\theta \neq \Delta\theta_0$ for $h = h_0$ if $t > t_0$.

This thought experiment shows that, if subsidence is present, $\Delta\theta$ is not only a function of h, but also of time. To solve Eq. 48, resulting in Eq. 69 through Eq. 67, separation of variables is applied. $\Delta\theta$ is expressed as a function of h, $f(h)$, and h is expressed as a function of t, $g(t)$. Equation 48 then results in $f(h)\frac{dh}{dt} = g(t)$ and, subsequently, $f(h)dh = g(t)dt$. This latter expression can be solved by simple integration. However, since $\Delta\theta$ is also dependent on time, $\Delta\theta = f(h,t)$. The resulting $f(h,t)\frac{dh}{dt} = g(t)$ could only be solved by separation of variables if $f(h,t)$ could be split into $f_1(h) \cdot f_2(t)$, which is not possible because h is dependent on t as well.

To the authors' knowledge, in the previous literature only Carson (1973) presents an analytical solution that accounts for subsidence. However, to arrive at his solution he assumes that $\Delta\theta$ scales linearly with h. Next to the influence of the initial conditions, they therefore directly ignore the dependence of $\Delta\theta$ on time. As such, this results in a first approximation of the boundary-layer height evolution rather than an exact solution.

4 Conclusions

The prognostic equations for a diurnal convective boundary layer are analytically solved. Compared to the most advanced solution in the literature, the results are expanded upon by including the effects of specific humidity. The resulting equations are an implicit expression for the boundary-layer height, due to the non-linear dependence of h on $\Delta\theta$, and explicit expressions for boundary-layer averaged scalars that are a function of the boundary-layer height and the time integral of their respective surface fluxes. As the ABL height cannot be directly derived from the implicit solution, an explicit simplification is presented that exactly captures the ABL height evolution for relatively large h. The differences between this expression and expressions for h of previous studies are clear for the cases under study. However, for relatively small h the mismatch between this simplification and the true boundary-layer height can be significant.

We therefore introduce an expression that enables us to determine the height at which a certain accuracy has been reached compared to the true boundary-layer height. To complete our analysis, a hybrid expression for h is derived. For this expression, the solution presented in the previous literature is substituted into the term of the implicit expression for h that becomes negligible for relatively large h. By doing so, an expression is obtained that represents the boundary-layer height evolution reasonably well for relatively small h and becomes the exact solution for larger h. Therefore, this expression could be used to predict the diurnal ABL height evolution without numerical solving the governing equations. As a result, evolutions of boundary-layer properties and dependencies of the height on other variables can be analytically determined, as demonstrated with our sensitivity analysis.

Sensitivity analyses by numerical solutions are always restricted to a limited amount of samples of the driving variable in question, while they are continuous expressions when using analytical solutions. As such, compared to previously obtained numerical solutions, the analytical solutions enable us to improve our understanding and discussion of the evolution of boundary-layer dynamics. This is very useful for research and educational purposes.

Here, we explored the dependence of h on the five driving variables identified from the exact implicit expression. Next to using sensitivity analyses, the evolution of the boundary-layer height is expressed with dimensionless groups. This expression clearly shows that the growth of the boundary layer is governed by the difference between the scaled time-integrated surface buoyancy flux and the relative strength of the initial virtual potential temperature jump compared to the free tropospheric virtual potential temperature profile. Possible applications for an analytical expression of the boundary-layer height evolution include calculating the potential temperature deficit and resulting latent and sensible heat fluxes (Raupach 2000), and analyzing the uncertainties in the determination of the CO2 budget that are associated with the boundary-layer dynamics (Pino et al. 2012).

Appendix A: Analytical Derivation

A1 Dependence of Potential Temperature on ABL Height

In this section the dependency of the mixed-layer slab averaged potential temperature, $\langle\theta\rangle$, and the potential temperature jump at the inversion, $\Delta\theta$, on the boundary-layer height are determined. First, the dependence of $\Delta\theta$ on h is derived. Based on Eqs. 1, 5 and 6,

$$\Delta\theta \frac{dh}{dt} = \beta \overline{w'\theta'}_0 \tag{48}$$
$$= \left(\frac{\beta}{1+\beta}\right) h \frac{d\langle\theta\rangle}{dt}.$$

Combined with Eq. 3, this results in

$$\Delta\theta \frac{dh}{dt} = \left(\frac{\beta}{1+\beta}\right) h \left(\gamma_\theta \frac{dh}{dt} - \frac{d\Delta\theta}{dt}\right),$$
$$(1+\beta)\,\Delta\theta \frac{dh}{dt} = \beta\gamma_\theta h \frac{dh}{dt} - \beta h \frac{d\Delta\theta}{dt}. \tag{49}$$

In this equation, the dependency on time can be removed by using $\frac{d\Delta\theta}{dt} = \frac{\partial\Delta\theta}{\partial h} \frac{dh}{dt}$ and dividing by $\frac{dh}{dt}$.

$$(1+\beta)\,\Delta\theta = \beta\gamma_\theta h - \beta h \frac{d\Delta\theta}{dh}, \tag{50}$$
$$\frac{d\Delta\theta}{dh} = \gamma_\theta - \left(\frac{1+\beta}{\beta}\right) \frac{\Delta\theta}{h}. \tag{51}$$

To solve this equation, a substitution is performed by $f \equiv \frac{\mathrm{d}\Delta\theta}{\mathrm{d}h}$, resulting in

$$f = \gamma_\theta - \left(\frac{1+\beta}{\beta}\right)\frac{\Delta\theta}{h}, \tag{52}$$

$$\frac{\mathrm{d}f}{\mathrm{d}h} = -\left(\frac{1+\beta}{\beta}\right)\left(-\frac{\Delta\theta}{h^2} + \frac{1}{h}\frac{\mathrm{d}\Delta\theta}{\mathrm{d}h}\right), \tag{53}$$

$$\frac{\mathrm{d}\Delta\theta}{\mathrm{d}h} = \frac{\Delta\theta}{h} - \left(\frac{\beta}{1+\beta}\right)h\frac{\mathrm{d}f}{\mathrm{d}h}. \tag{54}$$

Combined with Eq. 50 this leads to

$$\frac{\Delta\theta}{h} - \left(\frac{\beta}{1+\beta}\right)h\frac{\mathrm{d}f}{\mathrm{d}h} = \gamma_\theta - \left(\frac{1+\beta}{\beta}\right)\frac{\Delta\theta}{h},$$

$$\left(\frac{\beta}{1+\beta}\right)h\frac{\mathrm{d}f}{\mathrm{d}h} = -\gamma_\theta - \left(\frac{1+2\beta}{\beta}\right)\frac{\Delta\theta}{h}. \tag{55}$$

By using the relation from Eq. 52 it is found that

$$\left(\frac{\beta}{1+\beta}\right)h\frac{\mathrm{d}f}{\mathrm{d}h} = -\gamma_\theta + \left(\frac{1+2\beta}{\beta}\right)\left(\frac{\beta}{1+\beta}\right)(\gamma_\theta - f), \tag{56}$$

$$\beta h\frac{\mathrm{d}f}{\mathrm{d}h} = \beta\gamma_\theta - (1+2\beta)f. \tag{57}$$

This can be rewritten as

$$\frac{\mathrm{d}f}{f - \left(\frac{\beta}{1+2\beta}\right)\gamma_\theta} = -\left(\frac{1+2\beta}{\beta}\right)\frac{\mathrm{d}h}{h}, \tag{58}$$

$$\ln\left(f - \left(\frac{\beta}{1+2\beta}\right)\gamma_\theta\right) = -\left(\frac{1+2\beta}{\beta}\right)\ln(h) + c_1, \tag{59}$$

in which c_1 is a constant that is still undetermined. This results in

$$f - \left(\frac{\beta}{1+2\beta}\right)\gamma_\theta = c_2 h^{-\frac{1+2\beta}{\beta}}. \tag{60}$$

In this equation, $c_2 = e^{c_1}$. Combined with Eq. 52 it is found that

$$\left(\frac{1+\beta}{1+2\beta}\right)\gamma_\theta - \left(\frac{1+\beta}{\beta}\right)\frac{\Delta\theta}{h} = c_2 h^{-\frac{1+2\beta}{\beta}}, \tag{61a}$$

$$\frac{\Delta\theta}{h} = \left(\frac{\beta}{1+2\beta}\right)\gamma_\theta - \left(\frac{\beta}{1+\beta}\right)c_2 h^{-\frac{1+2\beta}{\beta}}. \tag{61b}$$

In total,

$$\Delta\theta = \left(\frac{\beta}{1+2\beta}\right)\gamma_\theta h + c_3 h^{-\frac{1+\beta}{\beta}}, \tag{62}$$

where $c_3 = -\left(\frac{\beta}{1+\beta}\right)c_2$. The value of c_3 can be derived by evaluating the initial state where $(t, h, \Delta\theta, \langle\theta\rangle) = (t_0, h_0, \Delta\theta_0, \langle\theta\rangle_0)$. It follows that

$$c_3 = h_0^{\frac{1+\beta}{\beta}}\left(\Delta\theta_0 - \left(\frac{\beta}{1+2\beta}\right)\gamma_\theta h_0\right) \tag{63}$$

and

$$\Delta\theta = \left(\frac{\beta}{1+2\beta}\right)\gamma_\theta h + \left(\Delta\theta_0 h_0^{\frac{1+\beta}{\beta}} - \left(\frac{\beta}{1+2\beta}\right)\gamma_\theta h_0^{\frac{1+2\beta}{\beta}}\right) h^{-\frac{1+\beta}{\beta}}. \quad (64)$$

By integrating Eq. 3 over time, the dependency of the mixed-layer averaged potential temperature, $\langle\theta\rangle$, on h is found.

$$\Delta\theta - \Delta\theta_0 = \gamma_\theta(h - h_0) - (\langle\theta\rangle - \langle\theta\rangle_0),$$
$$\langle\theta\rangle = \langle\theta\rangle_0 - \gamma_\theta h_0 + \Delta\theta_0 + \gamma_\theta h - \Delta\theta. \quad (65)$$

By substituting Eq. 64, this results in

$$\langle\theta\rangle = \langle\theta\rangle_0 - \gamma_\theta h_0 + \Delta\theta_0 + \left(\frac{1+\beta}{1+2\beta}\right)\gamma_\theta h - \left(\Delta\theta_0 h_0^{\frac{1+\beta}{\beta}} - \left(\frac{\beta}{1+2\beta}\right)\gamma_\theta h_0^{\frac{1+2\beta}{\beta}}\right) h^{-\frac{1+\beta}{\beta}}. \quad (66)$$

A2 Evolution of the Boundary-Layer Height

With the previously determined relations, the time evolution of the boundary-layer height is derived. Equations 48 and 64 combine to

$$\left(\left(\frac{\beta}{1+2\beta}\right)\gamma_\theta h + \left(\Delta\theta_0 h_0^{\frac{1+\beta}{\beta}} - \left(\frac{\beta}{1+2\beta}\right)\gamma_\theta h_0^{\frac{1+2\beta}{\beta}}\right) h^{-\frac{1+\beta}{\beta}}\right)\frac{dh}{dt} = \beta\overline{w'\theta'}_0, \quad (67)$$

$$\frac{d}{dt}\left(\left(\frac{\beta}{1+2\beta}\right)\frac{\gamma_\theta}{2}h^2 - \beta\left(\Delta\theta_0 h_0^{\frac{1+\beta}{\beta}} - \left(\frac{\beta}{1+2\beta}\right)\gamma_\theta h_0^{\frac{1+2\beta}{\beta}}\right) h^{-\frac{1}{\beta}}\right) = \beta\overline{w'\theta'}_0. \quad (68)$$

Integrating this equation over time results in

$$\left(\frac{\gamma_\theta}{2+4\beta}\right)(h^2 - h_0^2) - \left(\Delta\theta_0 h_0^{\frac{1+\beta}{\beta}} - \left(\frac{\beta}{1+2\beta}\right)\gamma_\theta h_0^{\frac{1+2\beta}{\beta}}\right)\left(h^{-\frac{1}{\beta}} - h_0^{-\frac{1}{\beta}}\right) = \int_{t_0}^{t}\overline{w'\theta'}_0 dt. \quad (69)$$

This is rewritten to the implicit analytical solution

$$h^2 - \left(\frac{2+4\beta}{\gamma_\theta}\right)\left(\Delta\theta_0 h_0^{\frac{1+\beta}{\beta}} - \left(\frac{\beta}{1+2\beta}\right)\gamma_\theta h_0^{\frac{1+2\beta}{\beta}}\right) h^{-\frac{1}{\beta}}$$
$$= h_0^2 - \left(\frac{2+4\beta}{\gamma_\theta}\right)\left(\Delta\theta_0 h_0 - \left(\frac{\beta}{1+2\beta}\right)\gamma_\theta h_0^2\right) + \left(\frac{2+4\beta}{\gamma_\theta}\right)\int_{t_0}^{t}\overline{w'\theta'}_0 dt. \quad (70)$$

A2.1 Limit for Large h

Equation 70 can be denoted as

$$h^2\left(1 - \left(\frac{2+4\beta}{\gamma_\theta}\right)\left(\Delta\theta_0 h_0^{\frac{1+\beta}{\beta}} - \left(\frac{\beta}{1+2\beta}\right)\gamma_\theta h_0^{\frac{1+2\beta}{\beta}}\right) h^{-\frac{1+2\beta}{\beta}}\right)$$
$$= h_0^2 - \left(\frac{2+4\beta}{\gamma_\theta}\right)\left(\Delta\theta_0 h_0 - \left(\frac{\beta}{1+2\beta}\right)\gamma_\theta h_0^2\right) + \left(\frac{2+4\beta}{\gamma_\theta}\right)\int_{t_0}^{t}\overline{w'\theta'}_0 dt. \quad (71)$$

For 'large' h, the term with $h^{-\frac{1+2\beta}{\beta}}$ on the l.h.s. can be neglected. This is the case if

$$h \gg \left[\left(\frac{2+4\beta}{\gamma_\theta} \right) \left(\Delta\theta_0 h_0^{\frac{1+\beta}{\beta}} - \left(\frac{\beta}{1+2\beta} \right) \gamma_\theta h_0^{\frac{1+2\beta}{\beta}} \right) \right]^{\frac{\beta}{1+2\beta}}. \tag{72}$$

For these situations, Eq. 71 simplifies to

$$h \approx \sqrt{ h_0^2 - \left(\frac{2+4\beta}{\gamma_\theta} \right) \left(\Delta\theta_0 h_0 - \left(\frac{\beta}{1+2\beta} \right) \gamma_\theta h_0^2 \right) + \left(\frac{2+4\beta}{\gamma_\theta} \right) \int_{t_0}^{t} \overline{w'\theta'}_0 dt } \tag{73}$$

The accuracy of this expression is dependent on the initial conditions. It can be derived that Eq. 73 is valid within an accuracy of α if

$$\begin{cases} h \geq (1-\alpha) \left(\left(\frac{2+4\beta}{\gamma_\theta} \right) \frac{\Delta\theta_0 h_0^{\frac{1+\beta}{\beta}} - \left(\frac{\beta}{1+2\beta} \right) \gamma_\theta h_0^{\frac{1+2\beta}{\beta}}}{\alpha(2-\alpha)} \right)^{\frac{\beta}{1+2\beta}} & \text{if} \quad \Delta\theta_0 > \left(\frac{\beta}{1+2\beta} \right) \gamma_\theta h_0, \\[4mm] h \geq (1+\alpha) \left(\left(\frac{2+4\beta}{\gamma_\theta} \right) \frac{\left(\frac{\beta}{1+2\beta} \right) \gamma_\theta h_0^{\frac{1+2\beta}{\beta}} - \Delta\theta_0 h_0^{\frac{1+\beta}{\beta}}}{\alpha(2+\alpha)} \right)^{\frac{\beta}{1+2\beta}} & \text{if} \quad \Delta\theta_0 < \left(\frac{\beta}{1+2\beta} \right) \gamma_\theta h_0, \end{cases}$$

where h is the boundary-layer height that is calculated using this simplified equation.

A3 Evolution of Scalars

Consider any scalar, ϕ, without sources and sinks in the boundary layer. These scalars include potential temperature, θ, specific humidity, q, and mixing ratios of inert chemical species (e.g., c_{CO_2}, c_{CH_4}). If the initial vertical profile is characterized by a constant value in the mixed layer, $\langle\phi\rangle_0$, a jump at the top of this layer, $\Delta\phi_0$, and a linear profile in the free troposphere aloft. If the increase with height in the free troposphere is expressed by the tropospheric lapse rate, γ_ϕ, and the surface flux is denoted as $\overline{w'\phi'}_0$, then a mass budget below the current boundary-layer height, $h(t)$, leads to

$$A \int_0^{h(t)} \phi_0(z)\,dz + \int_{t_0}^{t} A\overline{w'\phi'}_0 dt = A \int_0^{h(t)} \phi(z)\,dz, \tag{74}$$

where A is the surface area under consideration.

$$h\langle\phi\rangle_0 + \int_{h_0}^{h} \left(\Delta\phi_0 + \gamma_\phi(z-z_0) \right) dz + \int_{t_0}^{t} \overline{w'\phi'}_0 dt = h\langle\phi\rangle. \tag{75}$$

Therefore, if the initial profile, the current boundary-layer height and the surface exchange as function of time are known, the current mixed-layer averaged scalar is expressed as

$$\langle\phi\rangle = \langle\phi\rangle_0 + \frac{h-h_0}{h}\Delta\phi_0 + \frac{\gamma_\phi}{2}\frac{(h-h_0)^2}{h} + \frac{1}{h}\int_{t_0}^{t} \overline{w'\phi'}_0 dt. \tag{76}$$

A4 Including Specific Humidity Effects

If the specific humidity, q in kg kg^{-1}, is non-zero, the driving variable for convection is not the standard potential temperature, θ, but the virtual potential temperature, θ_v (Stull 1988).

$$\theta_v = \theta \left(1 + 0.61q\right), \tag{77}$$

$$\overline{w'\theta'_v} \approx 0.61 \,\overline{\theta}\,\overline{w'q'} + (1 + 0.61\,\overline{q})\,\overline{w'\theta'}, \tag{78}$$

and Eq. 5 is replaced by

$$\overline{w'\theta'_v}_h = -\beta \overline{w'\theta'_v}_0. \tag{79}$$

Similar to the potential temperature, it is assumed that the vertical profile of the specific humidity is constant in the mixed layer with a jump on top and a linear profile in the free tropospheric layer aloft. Similar to Eqs. 1, 2 and 3, q is governed by

$$\overline{w'q'}_h = -\frac{\mathrm{d}h}{\mathrm{d}t}\Delta q, \tag{80}$$

$$\frac{\mathrm{d}\,\langle q\rangle}{\mathrm{d}t} = \frac{\overline{w'\theta'}_0 - \overline{w'\theta'}_h}{h}, \tag{81}$$

$$\frac{\mathrm{d}\Delta q}{\mathrm{d}t} = \gamma_q \frac{\mathrm{d}h}{\mathrm{d}t} - \frac{\mathrm{d}\,\langle q\rangle}{\mathrm{d}t}. \tag{82}$$

These equations can be combined to find the governing equations for θ_v.

$$\begin{aligned}
\Delta\theta_v &= \theta_{v,\mathrm{FT}} - \langle\theta_v\rangle, \\
&= \theta_{\mathrm{FT}}\left(1 + 0.61q_{\mathrm{FT}}\right) - \langle\theta\rangle\left(1 + 0.61\,\langle q\rangle\right), \\
&= \left(\langle\theta\rangle + \Delta\theta\right)\left(1 + 0.61\left(\langle q\rangle + \Delta q\right)\right) - \langle\theta\rangle\left(1 + 0.61\,\langle q\rangle\right), \tag{83}
\end{aligned}$$

$$\Delta\theta_v = \Delta\theta + 0.61\left(\langle\theta\rangle\,\Delta q + \Delta\theta\,\langle q\rangle + \Delta\theta\Delta q\right). \tag{84}$$

Further, according to Eqs. 1, 80 and 78,

$$\begin{aligned}
\overline{w'\theta'_v}_h &= 0.61\,\langle\theta\rangle\,\overline{w'q'}_h + (1 + 0.61\,\langle q\rangle)\,\overline{w'\theta'}_h, \\
&= -0.61\,\langle\theta\rangle\,\Delta q\frac{\mathrm{d}h}{\mathrm{d}t} - (1 + 0.61\,\langle q\rangle)\,\Delta\theta\frac{\mathrm{d}h}{\mathrm{d}t}, \\
&= -\left(\Delta\theta + 0.61\left(\langle\theta\rangle\,\Delta q + \Delta\theta\,\langle q\rangle + \Delta\theta\Delta q\right) - 0.61\Delta\theta\Delta q\right)\frac{\mathrm{d}h}{\mathrm{d}t}. \tag{85}
\end{aligned}$$

In contrast to the case without moisture, an approximation has to be made to reach an analytical solution. By assuming that $|\Delta\theta\Delta q| \ll \Delta\theta_v$ ($|\Delta\theta| \sim |\Delta\theta_v|$ and Δq is of the order of 10^{-3} kg kg^{-1}) and using the expression for $\Delta\theta_v$ from Eq. 83, Eq. 85 becomes

$$\overline{w'\theta'_v}_h = -\Delta\theta_v\frac{\mathrm{d}h}{\mathrm{d}t}, \tag{86}$$

$$\frac{\mathrm{d}h}{\mathrm{d}t} = -\frac{\overline{w'\theta'_v}_h}{\Delta\theta_v}. \tag{87}$$

This is the first governing equation for θ_v. From Eqs. 2, 77, 78 and 81 the second governing equation follows:

$$\frac{d \langle \theta_v \rangle}{dt} = \frac{d (\langle \theta \rangle (1 + 0.61 \langle q \rangle))}{dt},$$

$$= (1 + 0.61 \langle q \rangle) \frac{d \langle \theta \rangle}{dt} + 0.61 \langle \theta \rangle \frac{d \langle q \rangle}{dt},$$

$$= (1 + 0.61 \langle q \rangle) \frac{\overline{w'\theta'}_0 - \overline{w'\theta'}_h}{h} + 0.61 \langle \theta \rangle \frac{\overline{w'q'}_0 - \overline{w'q'}_h}{h}, \tag{88}$$

$$\frac{d \langle \theta_v \rangle}{dt} = \frac{\overline{w'\theta'}_{v0} - \overline{w'\theta'}_{vh}}{h}. \tag{89}$$

Finally,

$$\gamma_{\theta_v} (z) = \frac{d\theta_{v,FT} (z)}{dz},$$

$$= \frac{d (\theta_{FT} (z) (1 + 0.61 \, q_{FT} (z)))}{dz},$$

$$= (1 + 0.61 \, q_{FT} (z)) \frac{d\theta_{FT} (z)}{dz} + 0.61\theta_{FT} (z) \frac{dq_{FT} (z)}{dz},$$

$$= (1 + 0.61 \, q_{FT} (z)) \gamma_\theta + 0.61\theta_{FT} (z) \gamma_q. \tag{90}$$

A second assumption that is made is that γ_{θ_v} is approximately constant with height, since $0.61 \, |q_{FT} (h) - q_{FT} (h_0)| \ll 1 + 0.61 \, q_{FT} (h)$ and $|\theta_{FT} (h) - \theta_{FT} (h_0)| \ll \theta_{FT} (h)$. Therefore,

$$\gamma_{\theta_v} = (1 + 0.61 \, q_{FT} (h_0)) \gamma_\theta + 0.61\theta_{FT} (h_0) \gamma_q. \tag{91}$$

By taking the derivative to time of Eq. 83,

$$\frac{d\Delta\theta_v}{dt} = \frac{d\theta_{v,FT}}{dt} - \frac{d \langle \theta_v \rangle}{dt},$$

$$= \frac{d\theta_{v,FT}}{dh} \frac{dh}{dt} - \frac{d \langle \theta_v \rangle}{dt}, \tag{92}$$

$$\frac{d\Delta\theta_v}{dt} = \gamma_{\theta_v} \frac{dh}{dt} - \frac{d \langle \theta_v \rangle}{dt}. \tag{93}$$

As Eqs. 86, 89, 93 and 79 replace Eqs. 1, 2, 3 and 5, the analytical solution for the boundary-layer height evolution is derived in a similar fashion as for the case without moisture. In accordance to Eq. 70, the implicit analytical solution is

$$h^2 - \left(\frac{2 + 4\beta}{\gamma_{\theta_v}}\right) \left(\Delta\theta_{v,0} h_0^{\frac{1+\beta}{\beta}} - \left(\frac{\beta}{1 + 2\beta}\right) \gamma_{\theta_v} h_0^{\frac{1+2\beta}{\beta}}\right) h^{-\frac{1}{\beta}}$$

$$= h_0^2 - \left(\frac{2 + 4\beta}{\gamma_{\theta_v}}\right) \left(\Delta\theta_{v,0} h_0 - \left(\frac{\beta}{1 + 2\beta}\right) \gamma_{\theta_v} h_0^2\right) + \left(\frac{2 + 4\beta}{\gamma_{\theta_v}}\right) \int_{t_0}^{t} \overline{w'\theta'}_{v0} dt, \tag{94}$$

while the approximation for 'large' h, based on Eq. 73, is

$$h \approx \sqrt{h_0^2 - \left(\frac{2 + 4\beta}{\gamma_{\theta_v}}\right) \left(\Delta\theta_{v,0} h_0 - \left(\frac{\beta}{1 + 2\beta}\right) \gamma_{\theta_v} h_0^2\right) + \left(\frac{2 + 4\beta}{\gamma_{\theta_v}}\right) \int_{t_0}^{t} \overline{w'\theta'}_{v0} dt}. \tag{95}$$

A5 Check on Bijection

When evaluating Eqs. 70 and 94, note that these expressions can be written as $f(h(t)) = g(t)$. To verify that $f(h(t))$ is an implicit analytical solution for $h(t)$, it has to be checked whether there is bijection: each value for $f(h)$ always corresponds to a unique value of h and for every value of h there is an existing value for $f(h)$ when $h > h_0$. This is the case if $f(h)$ is a continuous function and

$$\frac{\mathrm{d}f(h)}{h} > 0 \quad \text{for } h > h_0. \tag{96}$$

In the case of Eq. 94,

$$
\begin{aligned}
\frac{\mathrm{d}f(h)}{\mathrm{d}h} &= 2h + \left(\frac{2+4\beta}{\beta\gamma_{\theta_v}}\right)\left(\Delta\theta_{v,0}h_0^{\frac{1+\beta}{\beta}} - \left(\frac{\beta}{1+2\beta}\right)\gamma_{\theta_v}h_0^{\frac{1+2\beta}{\beta}}\right)h^{-\frac{1+\beta}{\beta}}, \\
&= \left(2\left(h^{\frac{1+2\beta}{\beta}} - h_0^{\frac{1+2\beta}{\beta}}\right) + \left(\frac{2+4\beta}{\beta\gamma_{\theta_v}}\right)\Delta\theta_{v,0}h_0^{\frac{1+\beta}{\beta}}\right)h^{-\frac{1+\beta}{\beta}}.
\end{aligned}
\tag{97}
$$

For $h > h_0$, $h^{-\frac{1+\beta}{\beta}} > 0$ and $h^{\frac{1+2\beta}{\beta}} > h_0^{\frac{1+2\beta}{\beta}}$. Additionally, β, γ_{θ_v} and $\Delta\theta_{v,0}$ have positive values. Therefore $\frac{\mathrm{d}f(h)}{h} > 0$ and Eqs. 70 and 94 are analytical implicit solutions for $h(t)$.

References

Betts AK (1973) Non-precipitating cumulus convection and its parameterization. Q J R Meteorol Soc 99:178–196. doi:10.1002/qj.49709941915

Carson DJ (1973) The development of a dry inversion-capped convectively unstable boundary layer. Q J R Meteorol Soc 99:450–467. doi:10.1002/qj.49709942105

Culf AD, Fisch G, Malhi Y, Nobre AD (1997) The influence of the atmospheric boundary layer on carbon dioxide concentrations over a tropical forest. Agric For Meteorol 85:149–158. doi:10.1016/S0168-1923(96)02412-4

de Bruin HAR (1983) A model for the priestley-taylor parameter α. J Clim Appl Meteorol 22:572–578. doi:10.1175/1520-0450(1983)022<0572:AMFTPT>2.0.CO;2

Driedonks AGM (1982) Sensitivity analysis of the equations for a convectively mixed layer. Boundary-Layer Meteorol 22:475–580. doi:10.1007/BF00124706

Ek MB, Holtslag AAM (2004) Influence of soil moisture on boundary layer cloud development. J Hydrometeorol 5:86–99. doi:10.1175/1525-7541(2004)005<0086:IOSMOB>2.0.CO;2

Garratt JR (1992) The atmospheric boundary layer. Cambridge University Press, Cambridge, UK

Lilly DK (1968) Models of cloud-topped mixed-layer under a strong inversion. Q J R Meteorol Soc 94:292–309. doi:10.1002/qj.49709440106

Ouwersloot HG et al (2012) Characterization of a boreal convective boundary layer and its impact on atmospheric chemistry during HUMPPA-COPEC-2010. Atmos Chem Phys 12:9335–9353. doi:10.5194/acp-12-9335-2012

Pino D, Vilà-Guerau de Arellano J, Peters W, Schröter J, van Heerwaarden CC, Krol MC (2012) A conceptual framework to quantify the influence of convective boundary layer development on carbon dioxide mixing ratios. Atmos Chem Phys 12:2969–2985. doi:10.5194/acp-12-2969-2012

Porporato A (2009) Atmospheric boundary-layer dynamics with constant bowen ratio. Boundary-Layer Meteorol 132:227–240. doi:10.1007/s10546-009-9400-8

Raupach MR (2000) Equilibrium evaporation and the convective boundary layer. Boundary-Layer Meteorol 96:107–142. doi:10.1023/A:1002675729075

Stensrud DJ (1993) Elevated residual layers and their influence on surface boundary-layer evolution. J Atmos Sci 50:2284–2293. doi:10.1175/1520-0469(1993)050<2284:ERLATI>2.0.CO;2

Stull RB (1988) An introduction to boundary layer meteorology. Kluwer, Dordrecht, 666 pp

Tennekes H (1973) A model for the dynamics of the inversion above a convective boundary layer. J Atmos Sci 30:558–567. doi:10.1175/1520-0469(1973)030<0558:AMFTDO>2.0.CO;2

van Driel R, Jonker HJJ (2011) Convective boundary layers driven by nonstationary surface heat fluxes. J Atmos Sci 68:727–738. doi:10.1175/2010JAS3643.1

van Heerwaarden CC, Vilà-Guerau de Arellano J, Gounou A, Guichard F, Couvreux F (2010) Understanding the daily cycle of evapotranspiration: a method to quantify the influence of forcings and feedbacks. J Hydrometeorol 11:1405–1422. doi:10.1175/2010JHM1272.1

van Stratum BJH et al (2012) Case study of the diurnal variability of chemically active species with respect to boundary layer dynamics during domino. Atmos Chem Phys 12:5329–5341. doi:10.5194/acp-12-5329-2012

Vilà-Guerau de Arellano J (2007) Role of nocturnal turbulence and advection in the formation of shallow cumulus over land. Q J R Meteorol Soc 133:1615–1627. doi:10.1002/qj.138

Vilà-Guerau de Arellano J, van den Dries K, Pino D (2009) On inferring isoprene emission surface flux from atmospheric boundary layer concentration measurements. Atmos Chem Phys 9:3629–3640. doi:10.5194/acp-9-3629-2009